Structurally Homologous All β-Barrel Proteins Adopt Different Mechanisms of Folding

Thiagarajan Srimathi,* Thallampuranam Krishnaswamy S. Kumar,[†] Karuppanan Muthusamy Kathir,*
Ya-Hui Chi,* Sampath Srisailam,* Wann-Yin Lin,[‡] Ing-Ming Chiu,[§] and Chin Yu[†]

*Department of Chemistry, National Tsing Hua University, Hsinchu, Taiwan; [†]Department of Chemistry and Biochemistry,
University of Arkansas, Fayetteville, Arkansas 72701; [‡]Department of Chemistry, National Taiwan University,
Taipei, Taiwan; and [§]Department of Internal Medicine, The Ohio State University, Columbus, Ohio 43210

ABSTRACT   Acidic fibroblast growth factors from human (hFGF-1) and newt (nFGF-1) (*Notopthalamus viridescens*) are 16-kDa, all β-sheet proteins with nearly identical three-dimensional structures. Guanidine hydrochloride (GdnHCl)-induced unfolding of hFGF-1 and nFGF-1 monitored by fluorescence and far-UV circular dichroism (CD) shows that the FGF-1 isoforms differ significantly in their thermodynamic stabilities. GdnHCl-induced unfolding of nFGF-1 follows a two-state (Native state to Denatured state(s)) mechanism without detectable intermediate(s). By contrast, unfolding of hFGF-1 monitored by fluorescence, far-UV circular dichroism, size-exclusion chromatography, and NMR spectroscopy shows that the unfolding process is noncooperative and proceeds with the accumulation of stable intermediate(s) at 0.96 M GdnHCl. The intermediate (in hFGF-1) populated maximally at 0.96 M GdnHCl has molten globule-like properties and shows strong binding affinity to the hydrophobic dye, 1-Anilino-8-naphthalene sulfonate (ANS). Refolding kinetics of hFGF-1 and nFGF-1 monitored by stopped-flow fluorescence reveal that hFGF-1 and nFGF-1 adopts different folding mechanisms. The observed differences in the folding/unfolding mechanisms of nFGF-1 and hFGF-1 are proposed to be either due to differential stabilizing effects of the charged denaturant ($Gdn^+ Cl^-$) on the intermediate state(s) and/or due to differences in the structural interactions stabilizing the native conformation(s) of the FGF-1 isoforms.

INTRODUCTION

Understanding the mechanism of how a polypeptide achieves its unique native conformation is one of the main challenges in structural biology (Rothwarf and Scheraga, 1996; Dill, 1990; Dinner et al., 2000; Fersht and Daggett, 2002; Matthews, 1993). Protein folding obviously is not a simple stochastic process (Kim and Baldwin, 1982; Levinthal, 1968). Folding is believed to be a complicated and directed process involving a definite sequence of intermediates with decreasing Gibbs energies (Edgcomb and Murphy, 2000; Kiefhaber, 1995). Classically, the presence of defined intermediates on folding pathway(s) is predicted to overcome the time-space problem (Shakhnovich et al., 1996). Characterizing these intermediates will be of considerable value in understanding the events and the dominant forces involved in protein folding.

Recently, several new models for the folding process involving energy landscapes have been described (Chan and Dill, 1994; Dill and Chan, 1997; Onuchic et al., 1995). These models propose that protein folding proceeds through multiple routes starting from a large set of unfolded conformations and eventually culminating in the formation of unique native state conformation (Baldwin, 1995; Fersht et al., 1994). Some of these folding routes might involve the

formation of completely or partially unfolded structures before the native conformation is realized (Baldwin, 1995; Fersht et al., 1994; Ptitsyn, 1998).

The classical and the new models of folding can be investigated experimentally by comparing the folding mechanisms of structurally homologous proteins (Dalessio and Ropson, 2000; Gunasekaran et al., 2001; Hooke et al., 1994; Martinez et al., 1998). The classical model envisages that if the native states of proteins adopt similar structural folds, the structures of the intermediates occurring in the folding pathway(s) should also be conserved (Baldwin, 1995; Fersht et al., 1994; Kuwajima, 1989). On the other hand, the new models predict that structurally homologous proteins could fold via different folding pathway(s) to finally reach the same/similar native conformation (Baldwin, 1995). It is in this context in the present study that we compare the folding mechanisms of two structurally homologous acidic fibroblast growth factors isolated from the human (hFGF-1) and newt (nFGF-1, *Notophalamus viridescens*) sources.

Both hFGF-1 and nFGF-1 are ~16-kDa, all β-barrel proteins lacking in disulfide bonds (Arunkumara et al., 2000; Chi et al., 2000, 2001; Samuel et al., 2001, 2000; Srisailam et al., 2002a). The FGF-1 isoforms (hFGF-1 and nFGF-1) share ~80% homology in their primary amino acid sequence (Arunkumara et al., 2000; Srisailam et al., 2002b) (Fig. 1). hFGF-1 and nFGF-1 are structurally homologous (with a RMSD of ~1.0 Å for the superimposed backbone atoms), and the secondary structural elements in FGF-1 isoforms include 12 β-strands arranged antiparallely into a β-trefoil architecture (Arunkumar et al., 2002; Blaber et al., 1996; Ogura et al., 1999; Pineda-Lucena et al., 1996) (Fig. 2). In

```
hFGF-1    KKPKLLYCSNGGHFLRILPDGTVDGTRDRSDQHIQLQLSAESVGE
nFGF-1    QKPKLLYCSNGGYFLRIFPDGKVDGTRDRSDPYIQLQ FYAESVGE


hFGF-1    VYIKSTETGQYLAMDTDGLLYGSQTPNEECLFLERLEENHYNTYI
nFGF-1    VYIKSLETGQYLAMDSDGQLYASQSPS EECLFLERLEENNYNTYK


hFGF-1    SKKHAEKNWFVGLKKNGSCKRGPRTHYGQKAILFLPLPVSSD
nFGF-1    SKVHADKDWFVGIKKN GKTKPGSRTHFGQKAILFLPLPVSSD
```

FIGURE 1 Amino acid sequences of hFGF-1 and nFGF-1. The amino acids that differ in both the FGF-1 isoforms are shown in bold.

the present study, we investigate the events in the guanidine hydrochloride (GdnHCl)-induced folding/unfolding pathway(s) of hFGF-1 and nFGF-1. It is observed that, despite the high structural homology, the folding mechanisms of hFGF-1 and nFGF-1 are distinctly different.

MATERIALS AND METHODS

Ingredients for the Luria Broth were obtained from AMRESCO (Solan, OH). Aprotinin, pepstatin, leupeptin, Phenylmethylsulfonylfluoride (PMSF), Triton X-100, 1-Anilino-8-naphthalene sulfonate (ANS, magnesium salt), and β-mercaptoehanol were obtained from Sigma Chemical (St. Louis, MO). Guanidine hydrochloride (ultra pure) was purchased from Merck (Darmstadt, Germany). Heparin-sepharose was procured from Amersham-Pharmacia (Piscataway, NJ). All other chemicals used were of high quality analytical grade. Unless specified, all solutions were made in 100 mM phosphate buffer.

Protein purification

hFGF-1 and nFGF-1 were expressed in *Escherichia coli* BL21 (DE3)pLys bearing the recombinant plasmid pET20a. Recombinant hFGF-1 and nFGF-1 expressed in *E. coli* were purified on a heparin-sepharose affinity column using a stepwise sodium chloride gradient (0–0.85–1.5 M). Desalting of the purified proteins was achieved by ultra-filtration using an Amicon (Pharmacia, Uppsala, Sweden) setup. The purity of the proteins was assessed using SDS-PAGE. The homogeneity was confirmed by ES-Mass analysis.
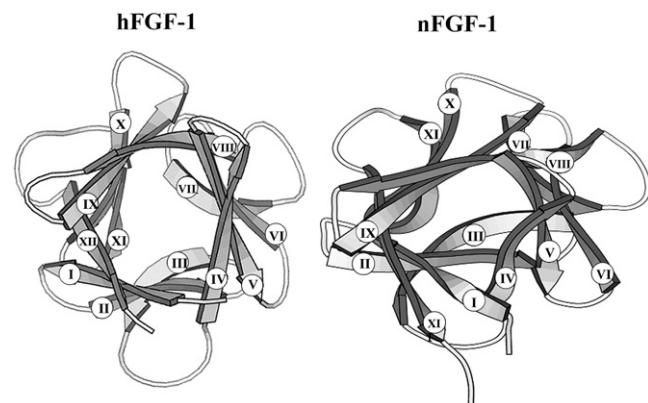

FIGURE 2 MOLSCRIPT representation of the three-dimensional structures of hFGF-1 and nFGF-1. The secondary structural elements in both the FGF-1 isoforms include 12 β-strands (labeled with *Roman numbers*) arranged into a β-barrel architecture.

Preparation of isotope enriched FGF-1

[15]N isotope labeling (of hFGF-1 and nFGF-1) was achieved using M9 minimal medium containing 100 mg/L [15]NH$_4$Cl. The expression host strain *E. coli* BL21(DE3)pLys is a vitamin B1 deficient host and hence the medium was supplemented with thiamin (vitamin B1). The protein yields were in the range of 20–25 mg/L. Purification procedure was the same as that explained earlier. The extent of labeling was verified by ES-Mass analysis and the isotope incorporation was found to be more than 95%.

GdnHCl-induced denaturation

Equilibrium unfolding of hFGF-1 was monitored by fluorescence and circular dichroism (CD) measurements as a function of GdnHCl concentration. Fluorescence spectra were measured using a Hitachi F-2500 fluorimeter at 2.5- or 10-nm resolution, using an excitation wavelength of 295 nm. All fluorescence measurements were made using a protein concentration of 100 μg/ml. The sample temperature was maintained at 25°C using a Neslab RTE-110 circulating water bath.

Circular dichroism spectra were measured using a Jasco J720 spectropolarimeter. CD spectra were collected with the slit width set to 1 nm, a response time of 1 s, and a scan speed of 20 nm/min. Each spectrum was an average of at least five scans. Secondary structure measurements were made at 225 nm with protein concentrations of 50 μM in a 1-cm path length cuvette.

Size-exclusion chromatography

All gel filtration experiments were carried out at 25°C on a superdex-100 column using an AKTA FPLC device (Amersham Pharmacia Biotech). The column was equilibrated with 2 bed vol of the buffer (100 mM phosphate buffer (pH 7.2) containing 100 mM ammonium sulfate) containing appropriate concentrations of GdnHCl. The flow rate of the eluent was set at 1 ml/min. Protein peaks were detected by their 280-nm absorbance. The concentration of the protein used was ~1 mg/ml.

Stopped-flow fluorescence

Kinetic measurements of protein refolding or unfolding were performed using a SF-61 stopped-flow spectrofluorimeter (Hi-Tech Scientific, Salisbury, UK). For measuring changes in the intrinsic tryptophan fluorescence (of Trp[121]) at different concentrations of GdnHCl, an excitation wavelength of 280 nm was routinely used with a monochromater slit width of 4 nm. All folding and unfolding reactions were performed at 25°C. Unfolding reactions involved mixing the proteins (hFGF-1 and nFGF-1) with 10-fold excess of GdnHCl to yield a final protein concentration of ~0.06 μM. The kinetics associated with refolding involved mixing 1 vol of unfolded protein with 10 vol of the refolding buffer (100 mM phosphate buffer (pH 7.2) containing 100 mM ammonium sulfate). The kinetics data were analyzed by plotting the refolding and unfolding rates as a function of denaturant concentration in semilogarithmic plots (Chevron plots) as per the following equations:

$$\ln k_{\mathrm{u}} = \ln k_{\mathrm{uw}} + m_{\mathrm{u}}[D]$$
$$\ln k_{\mathrm{f}} = \ln k_{\mathrm{fw}} + m_{\mathrm{f}}[D],$$

where k_{u} and k_{f} represent the observed rate constants for the unfolding and refolding reactions in various concentrations of the denaturant ($[D]$), respectively. k_{uw} and k_{fw} are the rate constants of unfolding and refolding extrapolated to 0 denaturant concentration. m_{u} and m_{f} are slopes of the unfolding and refolding reactions.

NMR spectroscopy

All NMR experiments were carried out on a Bruker DMX 600-MHz and

a Varian Inova 500-MHz spectrometer at 25°C. An inverse probe with a self-shielded z-gradient was used to obtain all gradient-enhanced ^{1}H-^{15}N HSQC spectra (Palmer et al., 1991). ^{15}N decoupling during acquisition was accomplished using the GARP sequence (Shaka et al., 1985). A total of 2048 complex data points were collected in the ^{1}H dimension of the ^{1}H-^{15}N HSQC experiments. In the indirect ^{15}N dimension of the spectra, 512 complex data points were collected. The HSQC spectra were recorded at 32 scans at all concentrations of GdnHCl. The concentration of the protein sample used was 0.5 mM in 95% H$_2$O and 5% D$_2$O (containing 100 mM phosphate and 100 mM ammonium sulfate). ^{15}N chemical shifts were referenced using the consensus ratio of 0.0101329118 (Wishart et al., 1995). All spectra were processed on a Silicon Graphics workstation using XWINNMR and Aurelia softwares. The GdnHCl-induced unfolding was monitored by the disappearance of the crosspeaks (that solely correspond to the native state of the protein) using the procedure reported by van Mierlo et al. (2000). Crosspeak volumes instead of crosspeak intensities were determined to avoid artifacts arising (due to line broadening effect with increase in the viscosity of the solvent) upon addition of GdnHCl.

Hydrogen-deuterium (H/D) exchange

The native proteins (hFGF-1 and nFGF-1) were lyophilized (1.5 mM in 0.5 ml buffer containing 100 mM phosphate, 100 mM ammonium sulfate, pH 6.0) and dissolved in 0.5 ml D$_2$O, immediately before data collection.

^{1}H-^{15}N HSQC at different time points were collected on Bruker 600 MHz spectrometer. For the native hFGF-1 and nFGF-1, ^{1}H-^{15}N HSQC spectra were collected continuously for every 20 min for 2 days, every 1 h on the 3rd day and every 4 h on the 4th day. ^{1}H-^{15}N HSQC spectra were acquired up to 50,000 min with few time points in between. Amide proton delays were followed by measuring the crosspeak volumes in ^{1}H-^{15}N HSQC spectra. The crosspeak volume in the HSQC spectra collected at various refolding times were normalized based on the peak height of the Ile^{70} γ-methyl protons (at 0.2 ppm) in the 1D ^{1}H NMR spectra collected each time before acquiring the HSQC spectra. The time courses of change in proton occupancies were fitted to a single exponential decay ($y = A \exp^{-kt} + C$, where A is the amplitude of the phase, k is the apparent exchange rate constant, and C is the final amplitude) using the Levenberg-Marquardt nonlinear least squares method. All data analysis was performed using Kaleidagraph software (Synergy software, Philadelphia, PA).

RESULTS AND DISCUSSION

Equilibrium unfolding of hFGF-1 and nFGF-1

The fluorescence and far-UV circular dichroism spectra of hFGF-1 and nFGF-1 are similar (Arunkumar et al., 2002; Samuel et al., 2000). The fluorescence spectra of the FGF-1 isoforms are dominated by tyrosine fluorescence at 308 nm (Dabora et al., 1991; Sanz and Gimenez-Gallego, 1997) (Fig. 3 A, inset I). The fluorescence of the lone, conserved tryptophan (Trp^{121}) is significantly quenched in the native conformation(s). The quenching effect is attributed to the presence of proximal imidazole and pyrrole groups in their three-dimensional structures. However, the quenching effect is relieved upon unfolding, and the fluorescence spectra of the proteins (hFGF-1 and nFGF-1) in the unfolded state(s) show an emission maxima at around 350 nm (Fig. 3 A, inset I). The far-UV CD spectra of the FGF-1 isoforms show features typical of all β-barrel proteins. The far-UV CD spectra have a minima at ∼206 nm and maxima at 228 nm (Fig. 3 A, inset II). The minima at 206 nm is typically

observed in class II β-proteins (Venyaminov and Yang, 1996). The positive ellipticity band at 228 nm is a combination of contributions from secondary structure, including β-turns and loops in the protein, and from aromatic residues (Venyaminov and Yang, 1996; Woody and Dunker, 1996). In the denatured state, the positive CD band at 228 nm disappears (Fig. 3 A, inset II). Hence, the conformational changes occurring during unfolding in hFGF-1 and nFGF-1 could be reliably monitored using fluorescence and far-UV CD spectroscopy.

Guanidine hydrochloride-induced equilibrium unfolding curves of hFGF-1 and nFGF-1 monitored by steady state fluorescence and far-UV CD are shown in Fig. 3, A and B. Unfolding profile of hFGF-1 monitored by fluorescence shows that the protein begins to unfold beyond 0.5 M GdnHCl. Complete unfolding of the protein occurs at GdnHCl concentrations greater than 1.5 M (Fig. 3 A). The C_m (the concentration at which 50% of the protein molecules exist in the unfolded state(s)) and m (the measure of the cooperativity of the FGF-1 unfolding process) are estimated to be 0.9 ± 0.1 M and 4.7 ± 0.1 kcal mol^{-1} M^{-1}, respectively. The change in the free energy [ΔG (H$_2$O)] for the transition from the folded to the unfolded state(s) is 4.5 ± 0.1 kcal mol^{-1}. Interestingly, the GdnHCl-induced unfolding profile of hFGF-1 obtained by monitoring the ellipticity changes at 228 nm does not superimpose with that realized using fluorescence spectroscopy (Fig. 3). The C_m, m, and [ΔG (H$_2$O)] values calculated from the unfolding data obtained using far-UV CD are 1.8 ± 0.1 M, 3.6 ± 0.1 kcal mol^{-1} M^{-1}, and 6.5 ± 0.1 kcal mol^{-1}, respectively. Noncoincidence of the unfolding profiles obtained by two optical spectroscopic probes clearly indicates that the GdnHCl-induced unfolding of hFGF-1 is noncooperative and proceeds with the accumulation of stable equilibrium intermediate(s) (Samuel et al., 2000).

The GdnHCl-induced unfolding profile of nFGF-1 monitored by fluorescence and far-UV CD are nearly superimposable, implying that the unfolding of the protein (nFGF-1) follows a two-state (Native ↔ Denatured states) mechanism without the accumulation of stable intermediate(s) (Fig. 3 B). The C_m, m, and [ΔG (H$_2$O)] values estimated for the GdnHCl-induced unfolding of nFGF-1 are 1.6 ± 0.2 M, 3.8 ± 0.1 kcal mol^{-1} M^{-1}, and 6.1 ± 0.1 kcal mol^{-1}, respectively. In summary, the results discussed above reveal that despite the high degree of amino acid sequence and structural homology between hFGF-1 and nFGF-1, the GdnHCl-induced equilibrium unfolding pathways of these proteins appear to be significantly different.

Accumulation of equilibrium intermediate(s)

Size-exclusion chromatography is a useful technique to probe the intrinsic changes in the molecular dimensions of a protein upon addition of a ligand or under denaturant effect. This technique has been successfully used to identify
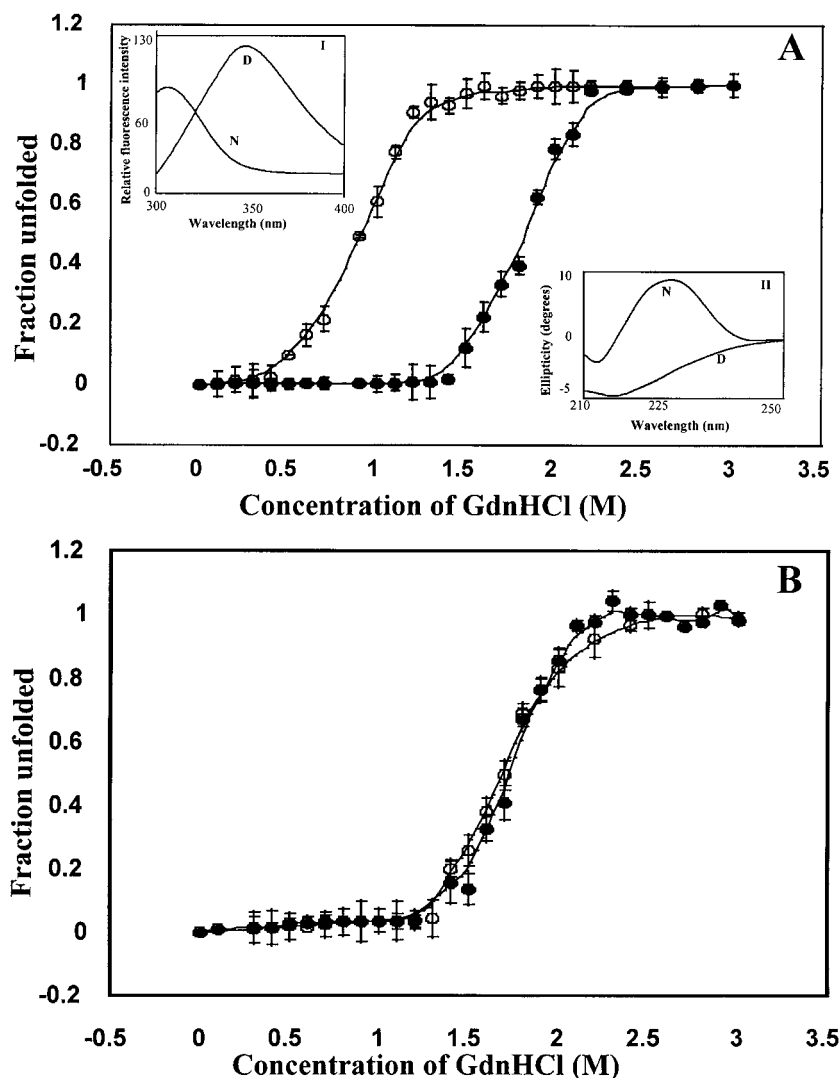
FIGURE 3 GdnHCl-induced unfolding profiles of hFGF-1 monitored by the changes in the 350-nm fluorescence (*open circles*) and 228-nm ellipticity changes (*closed circles*). The unfolding profiles monitored by both the spectroscopic probes do not overlap, implying the accumulation of stable equilibrium intermediates in the unfolding pathway of the protein. *Insets I* and *II* depict the fluorescence and far-UV CD spectra of hFGF-1 in the native (N) and unfolded (D) state(s), respectively. *B* depicts the GdnHCl-induced unfolding of nFGF-1 monitored by the changes in the 350-nm fluorescence and 228-nm ellipticity changes. The unfolding profiles monitored by the two spectroscopic techniques are nearly superimposable, indicating that the GdnHCl-induced unfolding of nFGF-1 follows a two-state (Native ↔ Denatured states) mechanism, without stable intermediate(s).

and characterize the hydrodynamic properties of equilibrium intermediate(s) in the folding/unfolding pathway(s) of proteins (Uversky, 1993). hFGF-1 in its native conformation (in 100 mM phosphate buffer (pH 7.2) containing 100 mM ammonium chloride) elutes as a single peak (retention time ~95 min) on a Superdex-100 SEC-FPLC column (Fig. 4 *A*). It is observed that the peak area corresponding to the native species (retention time ~95 min) progressively decreases with increase in the concentration of GdnHCl. Interestingly, one additional peak (apart from the native peak) with a retention time of ~87 min could also be observed in the FPLC profiles collected in the GdnHCl concentration range of 0.2–1.0 M (Fig. 4 *A*). The population of protein molecules representing the intermediate peak (retention time ~87 min) is maximal (~30%) at 1 M GdnHCl. Beyond 1.5 M GdnHCl, only a single peak (retention time ~78 min) corresponding to unfolded state(s) could be observed (Fig. 4 *A*). By contrast, the GdnHCl-induced unfolding of nFGF-1 monitored using size-exclusion chromatography does not provide any evidence of accumulation of intermediate state(s).

FPLC profiles show only peaks corresponding to the native (retention time ~95 min) and unfolded (retention time ~78 min) species at all concentrations of the denaturant (Fig. 4 *B*).

Significant differences could be observed in the GdnHCl unfolding profiles of hFGF-1 and nFGF-1 obtained by monitoring the changes in the area under the peak (retention time ~95 min) corresponding to the native state. The unfolding curve of hFGF-1 is biphasic (Fig. 4 *C*). Such multiphasic equilibrium unfolding profiles, monitored by size-exclusion chromatography, have been observed in several proteins and are attributed to the formation of stable equilibrium intermediates (Uversky, 1993). The first phase of unfolding extending between 0 and 1.0 M GdnHCl (in hFGF-1) appears to represent the equilibrium between the native (N) and intermediate (I) state(s) (Fig. 4 *C*). The transition from the intermediate (I) to the denatured state (D) (in hFGF-1) appears to be relatively sharp and occurs in the denaturant concentration range of 1.0–2.0 M. Interestingly, the GdnHCl-induced unfolding profile of nFGF-1 is mono-
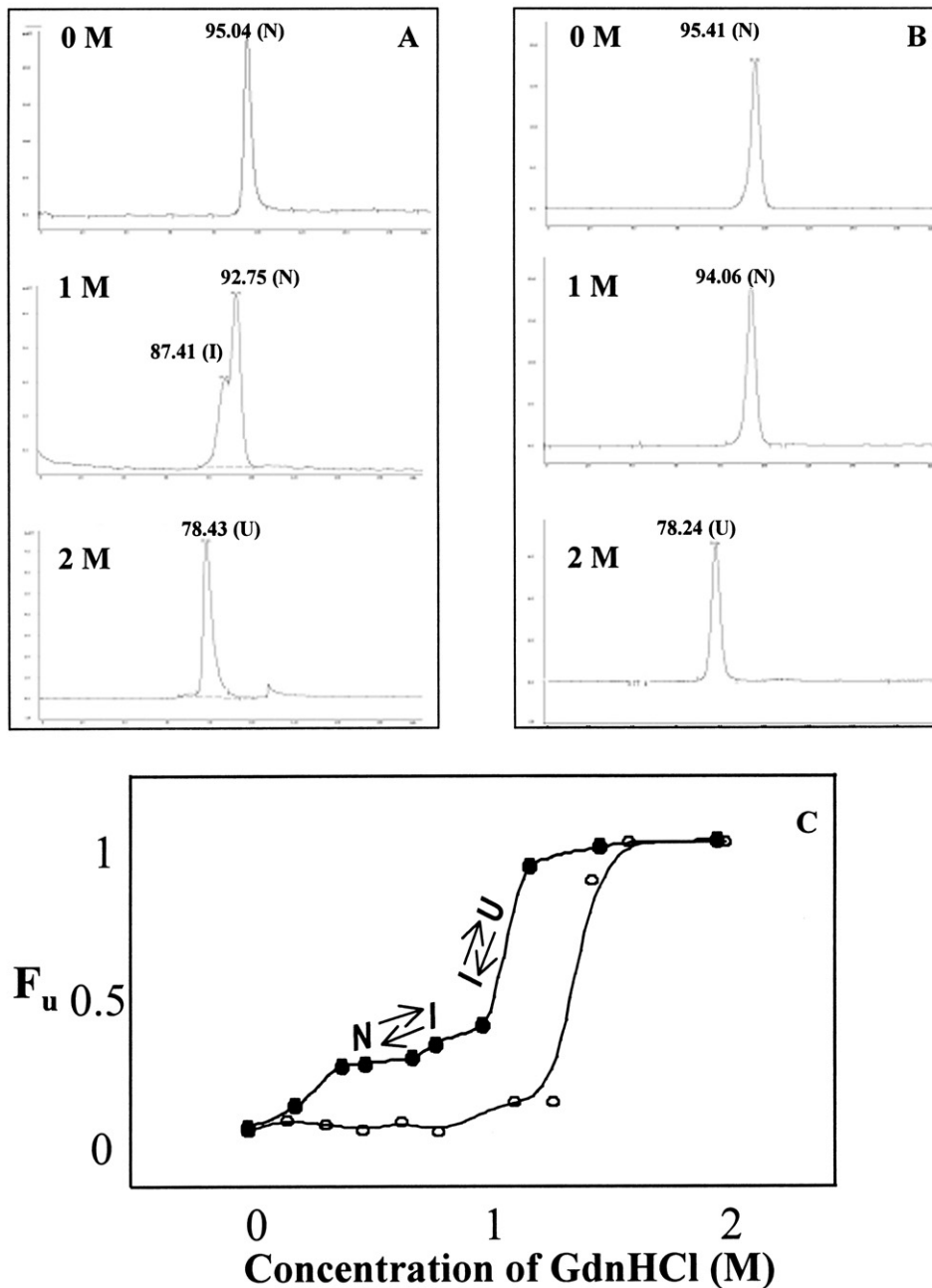
FIGURE 4 Elution profiles of hFGF-1 (A) and nFGF-1 (B) on SEC-FPLC at various concentrations of GdnHCl. The elution profile of hFGF-1 in 1M GdnHCl shows two peaks corresponding to the native (N) and intermediate (I) state(s) (A). However, the elution profiles of nFGF-1 at all concentrations of GdnHCl shows a peak corresponding to the native (N) or unfolded (U) state(s). C depicts the GdnHCl unfolding profiles of hFGF-1 (closed circle) and nFGF-1 (open circle) monitored by SEC-FPLC. The fraction of unfolded species formed was estimated from the decrease in the area corresponding to the native peak (retention time ∼95 min). It could be observed that the unfolding of nFGF-1 is cooperative, with only two detectable states (Native and Denatured state(s)). In contrast, the GdnHCl unfolding of hFGF-1 proceeds in two phases. In the first phase (0–1.0 M GdnHCl), the native to intermediate transition occurs. The intermediate to unfolded state(s) transition occurs in the second phase beyond 1.2 M GdnHCl.

phasic indicating that the protein unfolds by a two-state (Native to Denatured states) mechanism, without the accumulation of stable equilibrium intermediates (Fig. 4 C). Therefore, results of the size-exclusion chromatography experiments provide further evidence that the GdnHCl-induced equilibrium unfolding pathways of hFGF-1 and nFGF-1 are significantly different.

^{1}H-^{15}N HSQC spectrum serves as a fingerprint of the conformational states of a protein under given experimental conditions. The ^{1}H-^{15}N HSQC spectra of both hFGF-1 and nFGF-1 are well dispersed and all the crosspeaks have been unambiguously assigned (Figs. 5 A and 6 A). Hence, the

GdnHCl-induced conformational changes in the FGF-1 isoforms could be reliably monitored based on the ^{1}H-^{15}N chemical shift perturbation in the HSQC spectra obtained at various concentrations of the denaturant. ^{1}H-^{15}N HSQC spectra of nFGF-1 acquired below 0.2 M GdnHCl show no or very insignificant changes in the chemical shift value and in the volume of the ^{1}H-^{15}N crosspeaks. However, beyond 0.5 M GdnHCl, most of the crosspeaks show significant (^{1}H, ^{15}N) chemical shift perturbation (Fig. 5 A). ^{1}H-^{15}N HSQC spectra of nFGF-1 acquired at concentrations of the denaturant greater than 1.5 M are crowded and most of the crosspeaks are concentrated in a narrow region of the spectra (Fig.
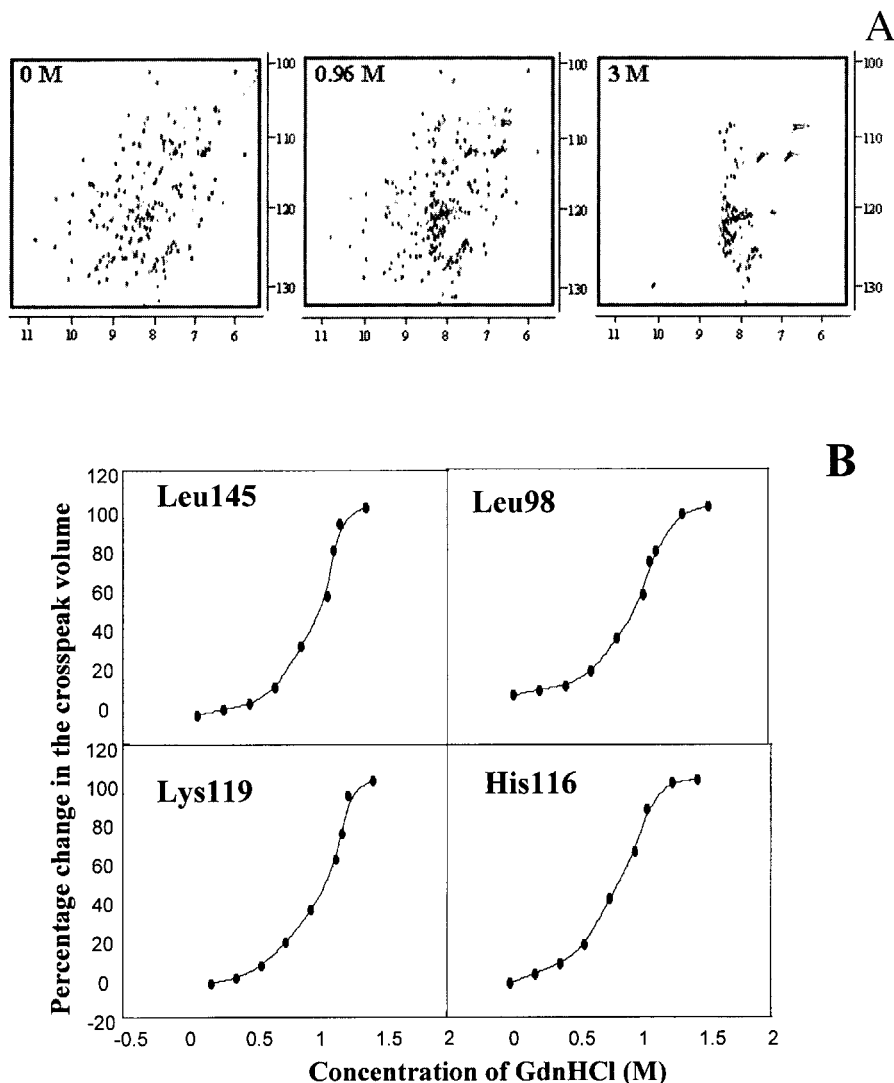
FIGURE 5 ^{1}H-^{15}N HSQC spectra of nFGF-1 at various concentrations of GdnHCl (*A*). *B* shows the unfolding profiles of nFGF-1 (at the individual amino acid level) monitored by the changes in the ^{1}H-^{15}N crosspeak volume. The unfolding profiles of Leu[98], His[116], Lys[119], and Leu[145] are sigmoidal, indicative of the cooperative (Native and Denatured states) nature of the GdnHCl-induced unfolding process.

5 *A*), implying that the protein (nFGF-1) under these conditions is in the unfolded state(s). Analysis of the ^{1}H-^{15}N HSQC spectra acquired at various concentrations of GdnHCl shows that there is a progressive decrease in the crosspeak volume with the increase in the denaturant concentration, reflecting depletion in the population of molecules in the native conformation (Fig. 5 *B*), as the concentration of the denaturant increases. Site-specific change(s) in the crosspeak volume as a function of the denaturant for most of the residues is sigmoidal, suggesting that the protein (nFGF-1) undergoes a cooperative, two-state (Native to Denatured state(s)) unfolding.

In hFGF-1, site-specific change(s) in crosspeak volume at various concentrations of GdnHCl could be monitored for 72 out of 126 HSQC crosspeaks (Fig. 6 *A*). These crosspeaks are isolated and distributed uniformly all over the ^{1}H-^{15}N HSQC spectrum. The unfolding profiles of many residues obtained by monitoring the change(s) in the crosspeak

volume (in the ^{1}H-^{15}N HSQC spectra) are sigmoidal and resemble typical denaturant-induced two-state (Native to Denatured state(s)) unfolding curves (Fig. 6 *B*). However, in contrast to nFGF-1, there are many residues located in various β-strands of hFGF-1 that show unfolding curves reminiscent of a three-state (Native $\leftrightarrow$ Intermediate $\leftrightarrow$ Denatured state(s)) unfolding process (Fig. 6 *B*). The unfolding curves of residues in hFGF-1 (such as Ile[144] and Gly[47]) show a prominent plateau in the GdnHCl concentration range of 0.8–1.0 M, indicative of the accumulation of stable intermediate species (Fig. 6 *B*). The nonuniform unfolding patterns of various residues suggest that hFGF-1 undergoes noncooperative unfolding in GdnHCl. In summary, the results discussed above clearly corroborate with those of fluorescence, far-UV CD, and size-exclusion chromatography and unambiguously suggest that despite being structurally homologous, hFGF-1 and nFGF-1 fold/unfold by significantly different mechanisms.
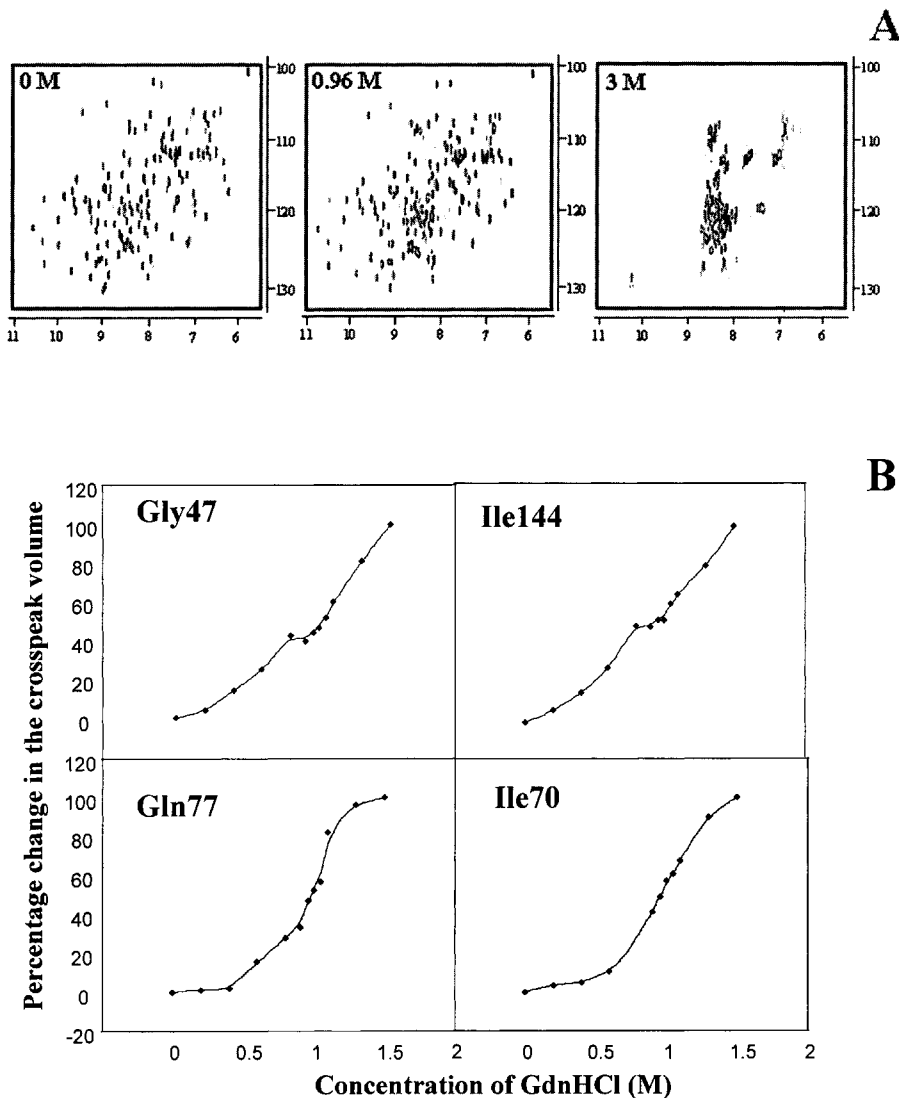
FIGURE 6 ^{1}H-^{15}N HSQC spectra of hFGF-1 at various concentrations of GdnHCl (A). B shows the unfolding profiles of hFGF-1 (at the individual amino acid level) monitored by the changes in the ^{1}H-^{15}N crosspeak volume. The unfolding profiles of residues Gly^{47} and Ile^{144} show a clear three-stage transition with a plateau between 0.5 and 1.0 M. In contrast, the unfolding curves of Ile^{70} and Gln^{77} appear to represent a two-state (native state to unfolded state(s)) transition.

1-Anilino-8-naphthalene sulfonate is a useful probe to identify stable equilibrium intermediates such as the molten globule (Schonbrunner et al., 1997; Semisotnov et al., 1991). ANS is a hydrophobic dye and has strong binding affinity to ordered solvent-exposed hydrophobic pockets in partially structured intermediates (such as the Molten Globule (MG) states). The dye exhibits weak binding affinity to the native and unfolded state(s) of proteins (Semisotnov et al., 1991). ANS binding affinity of nFGF-1 monitored by changes in the 520-nm fluorescence intensity at various concentrations of GdnHCl, shows no or insignificant changes in the emission (520-nm) intensity at all concentrations of the denaturant (Fig. 7). Similarly, the wavelength of maximal emission of the dye (ANS) also does not show appreciable change(s) (Fig. 7, inset A) as a function of the denaturant concentration, suggesting that the GdnHCl-induced unfolding of nFGF-1 does not involve the accumulation of stable equilibrium

intermediate(s) such as the MG state(s). By contrast, hFGF-1 exhibits strong binding affinity to ANS in the GdnHCl concentration range of 0.6–1.1 M (Fig. 7). The 550-nm emission intensity of the nonpolar dye in 0.96 M GdnHCl is more than twice that observed with hFGF-1 in its native state (Fig. 7, inset B). In addition, wavelength spectrum of ANS in the presence of the protein in 0.96 M GdnHCl shows that the emission maxima of the dye blue shifts by ~30 nm (from 520 to 490 nm). Increase in the GdnHCl concentration beyond 0.96 M is not only accompanied by a continuous red shift in the wavelength maximum, but also involves progressive decrease in the emission intensity (at 520 nm), indicating unfolding of the protein (hFGF-1). Therefore, the ANS binding experiments clearly reveal that the GdnHCl-induced equilibrium unfolding pathways of nFGF-1 and hFGF-1 are significantly different. The GdnHCl unfolding of nFGF-1 is cooperative (without the accumulation of
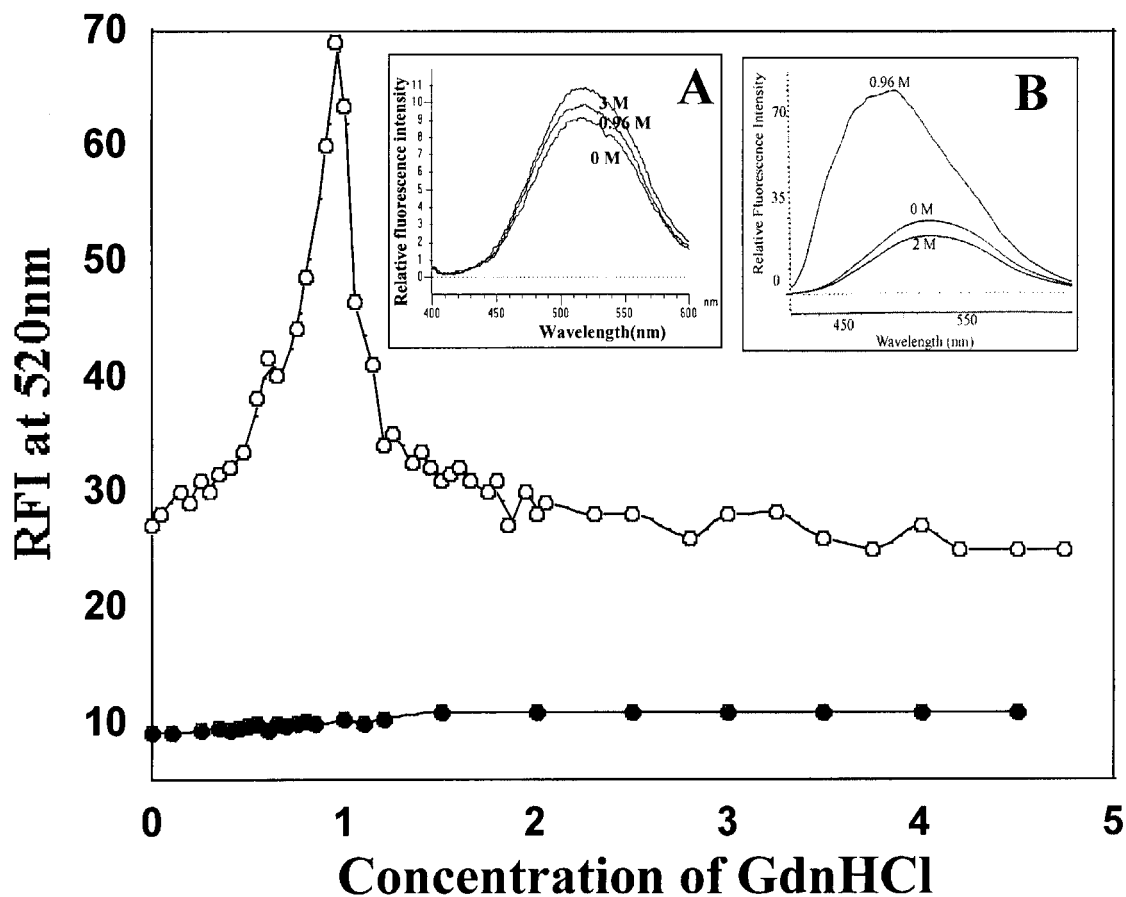
FIGURE 7   ANS binding of nFGF-1 (*closed circles*) and hFGF-1 (*open circles*) at various concentrations of GdnHCl. *Inset A* shows the fluorescence spectra of ANS in the presence of nFGF-1 at various concentrations of GdnHCl. No significant change(s) in the fluorescence intensity (at 520 nm) or wavelength of maximal fluorescence of the dye is observed (at any concentration of GdnHCl). These results suggest that no stable intermediate state(s) similar to the molten globule occurs in the GdnHCl-unfolding pathway of nFGF-1. In contrast, the ANS fluorescence (at 520 nm) increases by two-folds in 0.96 M GdnHCl implying the accumulation of the intermediate state(s) similar to the molten-globule state (*inset B*). The fluorescence spectrum of the dye also shows a 30-nm blue shift (as compared to the native state) in 0.96 M GdnHCl, indicating the binding of the dye (ANS) to solvent-exposed nonpolar surface(s) in the protein in the intermediate state(s) (at 0.96 M GdnHCl).

equilibrium intermediate(s)) but the unfolding of hFGF-1 involves the formation of at least a distinct stable intermediate (with characteristics of a MG state) that accumulates maximally in 0.96 M GdnHCl.

FGF-1 isoforms also differ in their kinetic refolding pathway(s)

It is known that in many proteins where an intermediate in equilibrium conditions is not found, the analysis of the refolding kinetics shows the unambiguous presence of intermediate(s). In this context, the refolding kinetics of nFGF-1 was examined using stopped-flow fluorescence by monitoring the changes in the tryptophan fluorescence (at 350 nm). hFGF-1 refolds from the 3 M GdnHCl denatured state slowly within a time span of ~30 s (Fig. 8 *A, inset*). The refolding curve best fits to a two exponential equation

yielding rate constants of $2.95 \pm 0.01 \times 10^{-1}$ and $1.16 \pm 0.01 \times 10^{-1}$ for the fast and slow phases, respectively. More than 85% of the amplitude change occurs during the fast phase of refolding. The slow phase observed in hFGF-1 is attributed to *cis–trans* proline isomerization (Samuel et al., 2001).

Fig. 8 depicts the GdnHCl dependence of the natural logarithm of the observed rate constants of folding/ unfolding (Chevron plot) of hFGF-1 and nFGF-1. The rate constant of the fast phase of refolding of nFGF-1 is observed to decrease linearly with the increase in the denaturant (GdnHCl) concentration (Fig. 8 *A*). Similarly, the unfolding rate of the protein (nFGF-1) increases linearly with increase in the GdnHCl concentration. The Chevron plot is V shaped and no prominent curvatures are observed in both the refolding and unfolding limbs of the plot, suggesting that the unfolding and refolding of nFGF-1 are cooperative and proceed without the accumulation of stable kinetic inter-
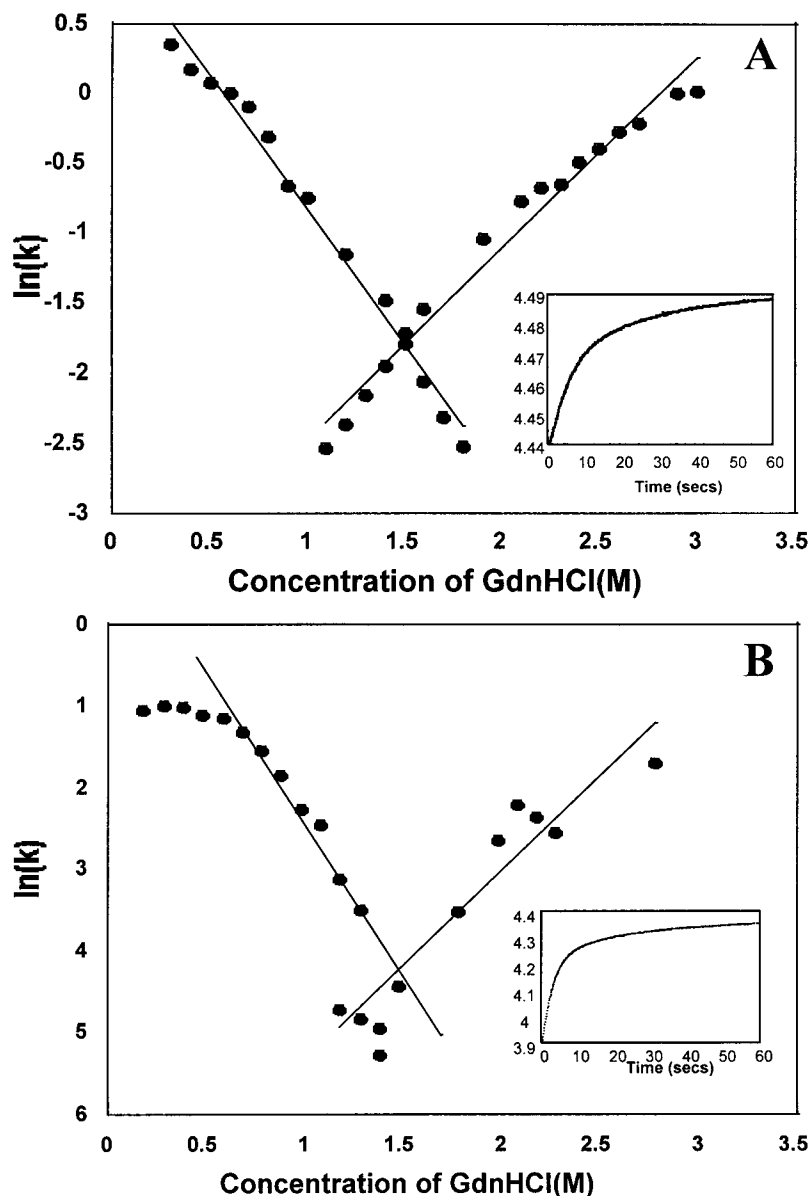
FIGURE 8 GdnHCl dependent folding kinetics (Chevron plot) of nFGF-1 (*A*) and hFGF-1 (*B*). The Chevron plot obtained for nFGF-1 is V shaped indicating that the folding and unfolding of the protein (nFGF-1) are cooperative, without the formation of stable kinetic intermediates. In contrast, the roll-over observed in Chevron plot of hFGF-1 (*B*) at low concentrations of GdnHCl, shows that the refolding of the protein involves the accumulation of stable kinetic intermediates. The *insets* in *A* and *B* indicate the refolding curves (monitored by changes in the 350-nm fluorescence) of nFGF-1 and hFGF-1, respectively.

mediate(s) (Fig. 8 *A*). It is pertinent to mention that the rate constant representing the slow phase (minor phase, and with amplitude ~10%) shows no denaturant dependence and is consistent with it being a rate-limiting proline isomerization event.

The refolding of hFGF-1 from its GdnHCl denatured state(s) is slow and complete refolding takes more than 30 s (Fig. 8 *B*). In contrast to nFGF-1, the Chevron plot of hFGF-1 exhibits a prominent curvature in the refolding limb, below 1.0 M GdnHCl (Fig. 8 *B*). Such a type of "roll-over" in the Chevron plot is a clear evidence for the accumulation of kinetic intermediate(s) at lower concentrations (<1.0 M) of the denaturant (Bhuyan and Udgaonkar, 1999; Parker and Marqusee, 1999). Therefore, it appears that the equilibrium intermediate(s) accumulated in 0.96 M GdnHCl also exists in the kinetic refolding pathway of hFGF-1.

The *m* value paradox

It would be interesting to understand the structural basis for the observed differences in the events of folding/unfolding of hFGF-1 and nFGF-1. The *m* value (an experimentally derived parameter) reflects the amount of newly exposed surface area upon denaturation of proteins using denaturants like urea or GdnHCl (Baskakov and Bolen, 1998). The *m* value represents the sensitivity of the protein to the chemically induced denaturation (Shortle and Meeker, 1986). Hence, the *m* value is a useful parameter to assess the cooperativity of a protein folding/unfolding reaction (Shirley et al., 1989). We compared the GdnHCl-induced unfolding profiles of hFGF-1 and nFGF-1 obtained by selectively monitoring the changes in the fluorescence (at 350 nm) of the sole conserved tryptophan residue in hFGF-1 and nFGF-1.

Comparison of the GdnHCl-induced unfolding curves of hFGF-1 and nFGF-1 reveals that these isoforms differ significantly in their thermodynamic stabilities (Fig. 9). hFGF-1 unfolds completely beyond 1.5 M GdnHCl. In contrast, complete unfolding of nFGF-1 occurs only beyond 2.5 M GdnHCl. The m values estimated for the GdnHCl-induced unfolding of hFGF-1 and nFGF-1 are estimated to be 4.7 $\pm$ 0.11 kcal mol^{-1} M^{-1} and 3.8 $\pm$ 0.095 kcal mol^{-1} M^{-1}, respectively. The estimated m values indicate that the GdnHCl-induced unfolding (to the denatured state(s)) of hFGF-1 is more cooperative than that of nFGF-1. These results are surprising and do not corroborate with the other data obtained in this study. As the GdnHCl-induced equilibrium unfolding of hFGF-1 proceeds via the accumulation of a stable intermediate state(s) (at around 0.96 M GdnHCl), the m value of hFGF-1 is expected to be less than that of nFGF-1 (which unfolds cooperatively). Such discrepancies in the m value have been reported in staphylococcal nuclease, and have been ascribed to basic problems of distinguishing between "compact denatured ensemble" that has residual structure from a "discrete intermediate state," existing between the native and a more fully denatured state(s) (Baskakov and Bolen, 1998; Carra et al., 1994; Carra and Privalov, 1995; Gittis et al., 1993; Shortle, 1995). In this context, it appears that the m value anomaly is possibly due to differences in the dimensional and thermodynamic characteristics of the denatured ensembles of nFGF-1 and hFGF-1 as detected by fluorescence spectroscopy (used to probe the GdnHCl-induced unfolding). Therefore, considerable caution needs to be exerted in the interpretation of the correlation between the estimated m values and the cooperativity of the protein folding/unfolding process.

Molecular basis for the difference(s) in the cooperativity of the folding/unfolding process of hFGF-1 and nFGF-1

Stabilization of the intermediate by GdnHCl

The complete unfolding of a protein involves the disruption of noncovalent intramolecular interactions within the protein and subsequent hydration of the backbone and amino acid side chains. Urea and GdnHCl are the most extensively used chemical denaturants, and they presumably exert their effect(s) by interacting with peptide bonds (Creighton, 1993; Mayo and Baldwin, 1993). These chemical denaturants are known to stabilize/destabilize equilibrium or kinetic intermediates occurring in the folding/unfolding pathways of proteins (Gianni et al., 2001; Gupta et al., 1996; Ropson et al., 1990). In addition, structure-based prediction methods for protein folding intermediates also revealed that the probability of accumulation of intermediates in folding/unfolding pathway(s) of proteins strongly depends on the stabilization of the charges on the protein in the intermediate state by the chemical denaturants (Xie and Freire, 1994). In this context, we examined the distribution of charges in the three-dimensional solution structures of hFGF-1 and nFGF-1.

Comparison of the three-dimensional structures of hFGF-1 and nFGF-1 reveals that the backbone folding of both these proteins are nearly identical (Fig. 2). The secondary structural elements in both the FGF-1 isoforms include 12 antiparallel β-strands arranged into a β-barrel architecture. The Stokes radius of FGF-1 isoforms measured by gel-filtration technique are also observed to be similar (15.76 $\pm$ 0.6 Å for hFGF-1 and 15.63 $\pm$ 0.8 Å for nFGF-1) (Ackers, 1967; Uversky, 1993). The solvent accessible hydrophobic
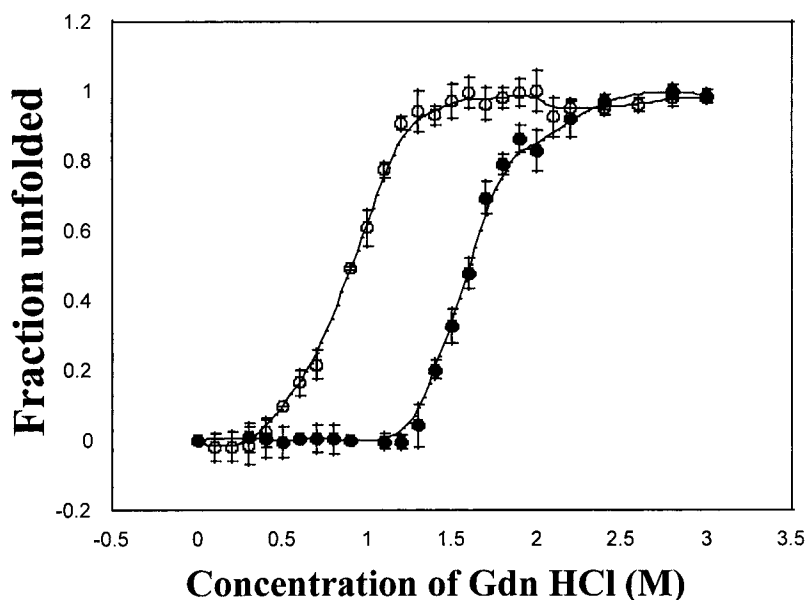
FIGURE 9 Comparison of the GdnHCl-induced unfolding profiles of hFGF-1 (*open circle*) and nFGF-1 (*closed circle*) monitored by changes in the tryptophan fluorescence. It could be observed that the slope of the unfolding curve (m value) of hFGF-1 is greater than that of nFGF-1. These results suggest that the GdnHCl-induced unfolding of hFGF-1 is more cooperative than that of nFGF-1.

contacts in hFGF-1 and nFGF-1 are mostly conserved with the exception of residues at the C-terminal end. The nonpolar side chains of residues located in the C-terminal segment in hFGF-1 (residues 115–130) such as Val[115], Phe[122], and Ile[125] are relatively more solvent exposed than in nFGF-1. In addition, the distribution of the positively charged residues on the surface of hFGF-1 and nFGF-1 are significantly different. A dense, positively charged cluster comprised of residues located in β-strand V, β-strand XI, β-strand XII, and residues in the loop between β-strands XI and XII (such as Arg[49], Arg[51], Arg[136], Lys[126], Lys[130], and Lys[142]) is found in the structure of hFGF-1 (Fig. 10 A). Unlike hFGF-1, the distribution of the positively charged residues is not continuous in nFGF-1 (Fig. 10 B). The side chains of the positively charged residues are relatively uniformly distributed on the surface of the nFGF-1 molecule and consequently the cationic cluster (observed in hFGF-1) is not very obvious. The differences in the distribution of the positively charged residues could be responsible for the observed difference(s) in the folding/unfolding mechanisms of hFGF-1 and nFGF-1. GdnHCl being a charged denaturant (contributing Gdn[+] and Cl^{−} ions) could stabilize the protein (hFGF-1) by effectively screening the repulsive forces among the closely positioned positively charged residues (in the cationic cluster) in the native and possibly in the intermediate state(s) (realized at 0.96 M GdnHCl) of hFGF-1. As a result both the native and intermediate states of hFGF-1 could be stabilized. In contrast, as nFGF-1 lacks prominent cationic clusters (Fig. 10 B), any intermediate(s) possibly formed in the folding/unfolding pathways are not influenced (stabilized) by GdnHCl. As a consequence, the equilibrium and kinetic folding/unfolding pathways of nFGF-1 follow a two-state mechanism with no detectable intermediate(s). Our proposal of the role of GdnHCl in the stabilization of intermediates in the folding/unfolding pathway of hFGF-1 appears meaningful because the urea (nonionic denaturant) induced equilibrium unfolding process of hFGF-1 was observed to be cooperative without the accumulation of stable intermediate(s) (data not shown).

Differences in the structural interactions stabilizing the native conformation

It is well known that the structural interactions in the native conformation not only govern the thermodynamic stability but also dictate the pathway(s) that a protein adopts during folding/unfolding (Johnson and Fersht, 1995). It is believed that residues that form the most stable core are the ones that importantly influence the crucial steps in protein folding (Bai et al., 1994; Kim and Woodward, 1993). Therefore, identification and comparison of the residues that contribute significantly to the stability of the structures of hFGF-1 and nFGF-1 would provide useful clues to understand the observed difference(s) in the mechanism(s) of folding/unfolding (of hFGF-1 and nFGF-1).
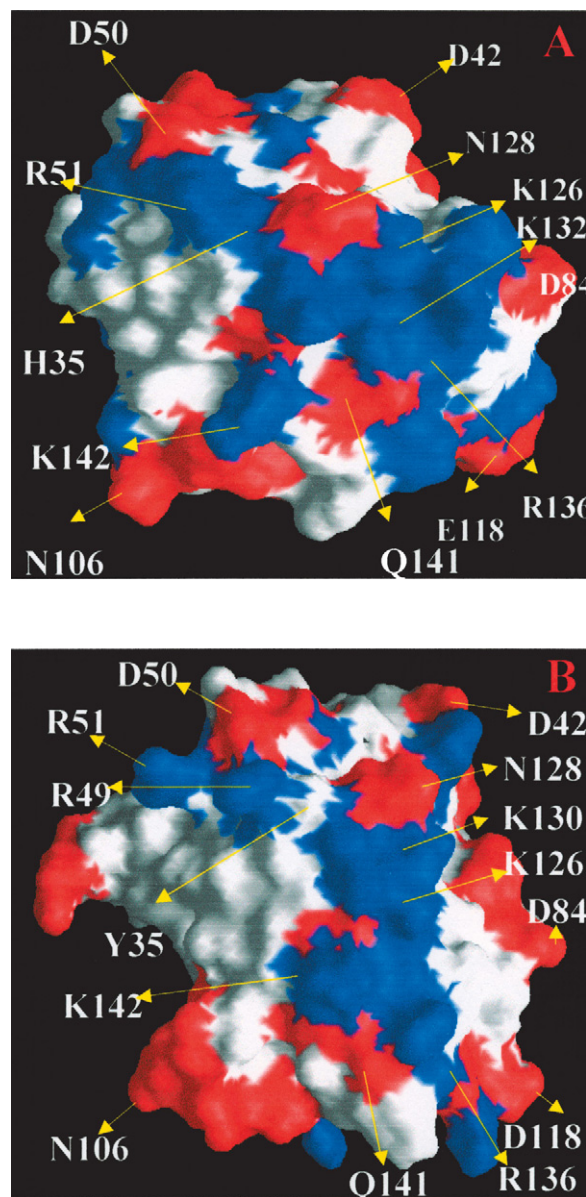

FIGURE 10 Surface charge distribution (*side view*) in the structures of hFGF-1 (*A*) and nFGF-1 (*B*). A dense, positively charged cluster comprising of residues His[35], Arg[51], Lys[126], Lys[132], Lys[136], and Lys[142] (indicated in *blue*) could be observed in the structure of hFGF-1. GdnHCl appears to stabilize the intermediate state (in hFGF-1 at 0.96 M GdnHCl) by screening the charge-charge repulsion among the closely positioned positively charged residues in the cationic cluster. In contrast, the positively charged residues in nFGF-1 are relatively uniformly distributed and consequently the cationic cluster is not dense. In the absence of a prominent cationic cluster (in nFGF-1), GdnHCl does not influence (stabilize) the equilibrium intermediates that possibly occur in the unfolding pathway.

Hydrogen-deuterium exchange monitored by two-dimensional NMR spectroscopy provides valuable information on the residues that contribute to the thermodynamic stability of a protein (Bai et al., 1994; Kim and Woodward, 1993). In this context, we monitored the H/D exchange (using ^{1}H-^{15}N HSQC spectra) of hFGF-1 and nFGF-1 under identical
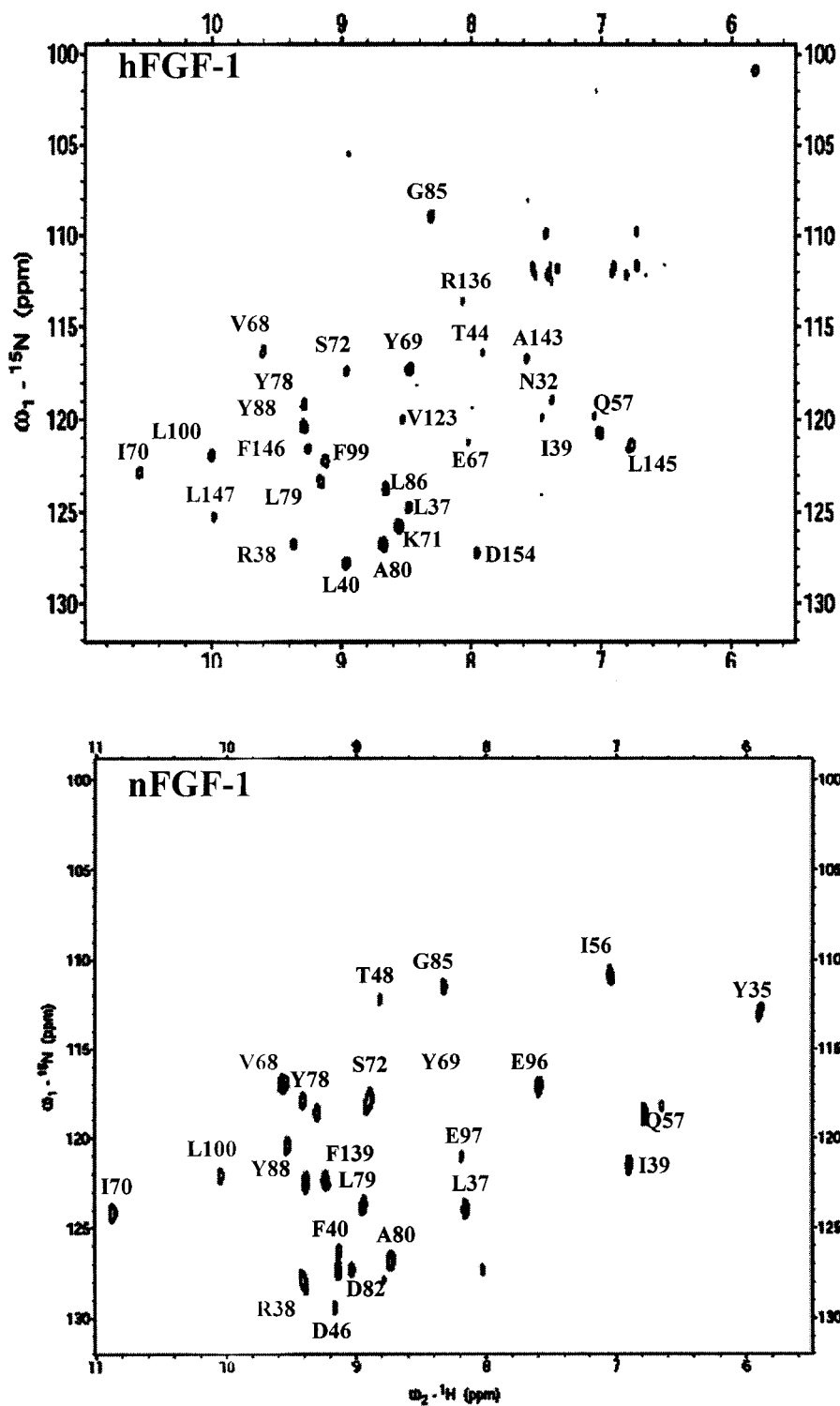
FIGURE 11 ^{1}H-^{15}N HSQC spectra of hFGF-1 and nFGF-1 in D$_2$O. The spectra were collected after about ~600 h of exchange. Some of the residues protected against H/D exchange (after ~600 h of exchange) are common in both hFGF-1 and nFGF-1, indicating that some of structural interactions stabilizing the structures of the FGF-1 isoforms are similar. However, there are several residues, which are strongly protected in nFGF-1 but not in hFGF-1 (or vice versa), indicating the differences in the residues contributing to the stable core in the two FGF-1 isoforms. The differences observed in the folding mechanism of hFGF-1 and nFGF-1 could be due to the differences in the structural interactions stabilizing their native conformation.

conditions for ~600 h. Comparison of the ^{1}H-^{15}N HSQC spectra of hFGF-1 and nFGF-1 acquired after ~600 h of exchange reveals that most of the crosspeaks have been completely exchanged out (Fig. 11 A). About 25 crosspeaks

are observed to be protected in both hFGF-1 and nFGF-1. Some of the residues (such as Leu[37], Arg[38], Leu[40], Glu[57], Val[68], Ile[70], Lys[71], Ser[72], Tyr[78], Ala[80], Leu[100], Leu[145], and Leu[147]) protected after ~600 h of exchange are common in

hFGF-1 and nFGF-1 (Fig. 11). This observation implies that some of the interactions stabilizing the structures of hFGF-1 and nFGF-1 are similar. About six amide protons that are prominently protected from exchange in nFGF-1 (collected after 600 h of H/D exchange) are observed to exchange rapidly in hFGF-1. These include the amide protons of Tyr[35], Asp[46], Thr[48], Ile[56], Glu[96], and Phe[139] (Fig. 11 B). Analysis of the three-dimensional structure of nFGF-1 shows that some of these residues (Thr[48], Ile[56], Tyr[35], and Phe[139]) are buried in the interior of the protein (nFGF-1) and are involved in hydrogen bonds (Arunkumar et al., 2002). Similarly, there are at least eight residues in hFGF-1 (Leu[40], Gln[57], Tyr[69], Tyr[78], Leu[86], Phe[97], Leu[145], and Asp[154] (Fig. 11 A) that are resistant to H/D exchange. These residues are completely exchanged out in nFGF-1 in the same time period (~600 h) of exchange (Fig. 11 B). Most of these residues are involved in short-range hydrogen bonds stabilizing the structure of the protein (hFGF-1). These results clearly indicate that although some of the interactions stabilizing the structures of hFGF-1 and nFGF-1 are common, there are several residues in the stable core, which are unique to each FGF-1 isoform. The difference(s) observed in the interactions stabilizing the native conformation (of hFGF-1 and nFGF-1) could also influence the stability of the intermediate(s) in their folding/unfolding pathway(s). At the present juncture, we are unable to precisely explain the molecular basis for the differences observed in folding/unfolding pathways of hFGF-1 and nFGF-1. However, we believe that the differences in the distribution of the charged residues and/or the differences in the nature of forces stabilizing the native conformation could be important factors in driving the structurally homologous proteins (hFGF-1 and nFGF-1) to adopt different folding/unfolding pathway(s). Work is currently underway to validate some of the proposals put forth in this study using several site-specific mutants of hFGF-1 and nFGF-1.

REFERENCES

Ackers, G. K. 1967. Molecular sieve studies of interacting protein systems. I. Equations for transport of associating systems. *J. Biol. Chem.* 242:3026–3034.

Arunkumar, A. I., T. K. S. Kumar, K. M. Kathir, S. Srisailam, H. M. Wang, P. S. Leena, Y. H. Chi, H. C. Chen, C. H. Wu, R. T. Wu, G. G. Chang, I. M. Chiu, and C. Yu. 2002. Oligomerization of acidic fibroblast growth factor is not a prerequisite for its cell proliferation activity. *Protein Sci.* 11:1050–1061.

Arunkumara, A. I., S. Srisailam, T. K. Kumar, K. M. Kathir, C. L. Peng, C. Chen, I. M. Chiu, and C. Yu. 2000. Letter to the editor: 1H, 13C and 15N chemical shift assignments of the acidic fibroblast growth factor from Notopthalmus viridescens. *J. Biomol. NMR.* 17:279–280.

Bai, Y., J. S. Milne, L. Mayne, and S. W. Englander. 1994. Protein stability parameters measured by hydrogen exchange. *Proteins.* 20:4–14.

Baldwin, R. L. 1995. The nature of protein folding pathways: the classical versus the new view. *J. Biomol. NMR.* 5:103–109.

Baskakov, I. V., and D. W. Bolen. 1998. Monitoring the sizes of denatured ensembles of staphylococcal nuclease proteins: implications regarding m values, intermediates, and thermodynamics. *Biochemistry.* 37:18010–18017.

Bhuyan, A. K., and J. B. Udgaonkar. 1999. Observation of multistate kinetics during the slow folding and unfolding of barstar. *Biochemistry.* 38:9158–9168.

Blaber, M., J. DiSalvo, and K. A. Thomas. 1996. X-ray crystal structure of human acidic fibroblast growth factor. *Biochemistry.* 35:2086–2094.

Carra, J. H., E. A. Anderson, and P. L. Privalov. 1994. Three-state thermodynamic analysis of the denaturation of staphylococcal nuclease mutants. *Biochemistry.* 33:10842–10850.

Carra, J. H., and P. L. Privalov. 1995. Energetics of denaturation and m values of staphylococcal nuclease mutants. *Biochemistry.* 34:2034–2041.

Chan, H. S., and K. A. Dill. 1994. Transition-states and folding dynamics of proteins and heteropolymers. *J. Chem. Phys.* 100:9238–9257.

Chi, Y., T. K. S. Kumar, I. M. Chiu, and C. Yu. 2000. 15N NMR relaxation studies of free and ligand-bound human acidic fibroblast growth factor. *J. Biol. Chem.* 275:39444–39450.

Chi, Y., T. K. S. Kumar, H. M. Wang, M. C. Ho, I. M. Chiu, and C. Yu. 2001. Thermodynamic characterization of the human acidic fibroblast growth factor: evidence for cold denaturation. *Biochemistry.* 40:7746–7753.

Creighton, T. E. 1993. Proteins: Structure and Molecular Properties. W. H. Freeman, New York.

Dabora, J. M., G. Sanyal, and C. R. Middaugh. 1991. Effect of polyanions on the refolding of human acidic fibroblast growth factor. *J. Biol. Chem.* 266:23637–23640.

Dalessio, P. M., and I. J. Ropson. 2000. Beta-sheet proteins with nearly identical structures have different folding intermediates. *Biochemistry.* 39:860–871.

Dill, K. A. 1990. Dominant forces in protein folding. *Biochemistry.* 29:7133–7155.

Dill, K. A., and H. S. Chan. 1997. From Levinthal to pathways to funnels. *Nat. Struct. Biol.* 4:10–19.

Dinner, A. R., A. Sali, L. J. Smith, C. M. Dobson, and M. Karplus. 2000. Understanding protein folding via free-energy surfaces from theory and experiment. *Trends Biochem. Sci.* 25:331–339.

Edgcomb, S. P., and K. P. Murphy. 2000. Structural energetics of protein folding and binding. *Curr. Opin. Biotechnol.* 11:62–66.

Fersht, A. R., and V. Daggett. 2002. Protein folding and unfolding at atomic resolution. *Cell.* 108:573–582.

Fersht, A. R., L. S. Itzhaki, N. F. elMasry, J. M. Matthews, and D. E. Otzen. 1994. Single versus parallel pathways of protein folding and fractional formation of structure in the transition state. *Proc. Natl. Acad. Sci. USA.* 91:10426–10429.

Gianni, S., M. Brunori, and C. Travaglini-Allocatelli. 2001. Refolding kinetics of cytochrome c(551) reveals a mechanistic difference between urea and guanidine. *Protein Sci.* 10:1685–1688.

Gittis, A. G., W. E. Stites, and E. E. Lattman. 1993. The phase transition between a compact denatured state and a random coil state in staphylococcal nuclease is first-order. *J. Mol. Biol.* 232:718–724.

Gunasekaran, K., S. J. Eyles, A. T. Hagler, and L. M. Gierasch. 2001. Keeping it in the family: folding studies of related proteins. *Curr. Opin. Struct. Biol.* 11:83–93.

Gupta, R., S. Yadav, and F. Ahmad. 1996. Protein stability: urea-induced versus guanidine-induced unfolding of metmyoglobin. *Biochemistry.* 35:11925–11930.

Hooke, S. D., S. E. Radford, and C. M. Dobson. 1994. The refolding of human lysozyme: a comparison with the structurally homologous hen lysozyme. *Biochemistry.* 33:5867–5876.

Johnson, C. M., and A. R. Fersht. 1995. Protein stability as a function of denaturant concentration: ther thermal stability of barnase in the presence of urea. *Biochemistry.* 34:6795–6804.

Kiefhaber, T. 1995. Kinetic traps in lysozyme folding. *Proc. Natl. Acad. Sci. USA.* 92:9029–9033.

Kim, K. S., and C. Woodward. 1993. Protein internal flexibility and global stability: effect of urea on hydrogen exchange rates of bovine pancreatic trypsin inhibitor. *Biochemistry.* 32:9609–9613.

Kim, P. S., and R. L. Baldwin. 1982. Specific intermediates in the folding reactions of small proteins and the mechanism of protein folding. *Annu. Rev. Biochem.* 51:459–489.

Kuwajima, K. 1989. The molten globule state as a clue for understanding the folding and cooperativity of globular-protein structure. *Proteins.* 6:87–103.

Levinthal, C. 1968. Are there pathways for protein folding? *J. Chem. Phys.* 65:44–45.

Martinez, J. C., M. T. Pisabarro, and L. Serrano. 1998. Obligatory steps in protein folding and the conformational diversity of the transition state. *Nat. Struct. Biol.* 5:721–729.

Matthews, C. R. 1993. Pathways of protein folding. *Annu. Rev. Biochem.* 62:653–683.

Mayo, S. L., and R. L. Baldwin. 1993. Guanidinium chloride induction of partial unfolding in amide proton exchange in RNase A. *Science.* 262:873–876.

Ogura, K., K. Nagata, H. Hatanaka, H. Habuchi, K. Kimata, S. Tate, M. W. Ravera, M. Jaye, J. Schlessinger, and F. Inagaki. 1999. Solution structure of human acidic fibroblast growth factor and interaction with heparin-derived hexasaccharide. *J. Biomol. NMR.* 13:11–24.

Onuchic, J. N., P. G. Wolynes, Z. Luthey-Schulten, and N. D. Socci. 1995. Toward an outline of the topography of a realistic protein-folding funnel. *Proc. Natl. Acad. Sci. USA.* 92:3626–3630.

Palmer, A. G., J. Cavanagh, P. E. Wright, and M. Rance. 1991. Sensitivity improvement in proton-detected 2-dimensional heteronuclear correlation NMR-spectroscopy. *J. Magn. Reson.* 93:151–170.

Parker, M. J., and S. Marqusee. 1999. The cooperativity of burst phase reactions explored. *J. Mol. Biol.* 293:1195–1210.

Pineda-Lucena, A., M. A. Jimenez, R. M. Lozano, J. L. Nieto, J. Santoro, M. Rico, and G. Gimenez-Gallego. 1996. Three-dimensional structure of acidic fibroblast growth factor in solution: effects of binding to a heparin functional analog. *J. Mol. Biol.* 264:162–178.

Ptitsyn, O. B. 1998. Protein folding and protein evolution: common folding nucleus in different subfamilies of c-type cytochromes? *J. Mol. Biol.* 278:655–666.

Ropson, I. J., J. I. Gordon, and C. Frieden. 1990. Folding of a predominantly beta-structure protein: rat intestinal fatty acid binding protein. *Biochemistry.* 29:9591–9599.

Rothwarf, D. M., and H. A. Scheraga. 1996. Role of non-native aromatic and hydrophobic interactions in the folding of hen egg white lysozyme. *Biochemistry.* 35:13797–13807.

Samuel, D., T. K. S. Kumar, K. Balamurugan, W. Y. Lin, D. H. Chin, and C. Yu. 2001. Structural events during the refolding of an all beta-sheet protein. *J. Biol. Chem.* 276:4134–4141.

Samuel, D., T. K. S. Kumar, T. Srimathi, H. Hsieh, and C. Yu. 2000. Identification and characterization of an equilibrium intermediate in the unfolding pathway of an all beta-barrel protein. *J. Biol. Chem.* 275:34968–34975.

Sanz, J. M., and G. Gimenez-Gallego. 1997. A partly folded state of acidic fibroblast growth factor at low pH. *Eur. J. Biochem.* 246:328–335.

Schonbrunner, N., G. Pappenberger, M. Scharf, J. Engels, and T. Kiefhaber. 1997. Effect of preformed correct tertiary interactions on rapid two-state tendamistat folding: evidence for hairpins as initiation sites for beta-sheet formation. *Biochemistry.* 36:9057–9065.

Semisotnov, G. V., N. A. Rodionova, O. I. Razgulyaev, V. N. Uversky, A. F. Gripas, and R. I. Gilmanshin. 1991. Study of the ''molten globule'' intermediate state in protein folding by a hydrophobic fluorescent probe. *Biopolymers.* 31:119–128.

Shaka, A. J., P. B. Barker, and R. Freeman. 1985. Computer-optimized decoupling scheme for wideband applications and low-level operation. *J. Magn. Reson.* 64:547–552.

Shakhnovich, E., V. Abkevich, and O. B. Ptitsyn. 1996. Conserved residues and the mechanism of protein folding. *Nature.* 379:96–98.

Shirley, B. A., P. Stanssens, J. Steyaert, and C. N. Pace. 1989. Conformational stability and activity of ribonuclease T1 and mutants. Gln25—Lys, Glu58—Ala, and the double mutant. *J. Biol. Chem.* 264:11621–11625.

Shortle, D. 1995. Staphylococcal nuclease: a showcase of m-value effects. *In* Advances in Protein Chemistry. D. S. Eisenberg, editor. Academic Press, New York. 217–247.

Shortle, D., and A. K. Meeker. 1986. Mutant forms of staphylococcal nuclease with altered patterns of guanidine hydrochloride and urea denaturation. *Proteins.* 1:81–89.

Srisailam, S., T. K. S. Kumar, T. Srimathi, and C. Yu. 2002a. Influence of backbone conformation on protein aggregation. *J. Am. Chem. Soc.* 124: 1884–1888.

Srisailam, S., H. M. Wang, T. K. S. Kumar, D. Rajalingam, V. Sivaraja, H. S. Sheu, Y. C. Chang, and C. Yu. 2002b. Amyloid-like fibril formation in an all beta-barrel protein involves the formation of partially structured intermediate(s). *J. Biol. Chem.* 277:19027–19036.

Uversky, V. N. 1993. Use of fast protein size-exclusion liquid chromatography to study the unfolding of proteins which denature through the molten globule. *Biochemistry.* 32:13288–13298.

van Mierlo, C. P., J. M. van den Oever, and E. Steensma. 2000. Apoflavodoxin (un)folding followed at the residue level by NMR. *Protein Sci.* 9:145–157.

Venyaminov, S. Y., and J. T. Yang. 1996. Determination of protein secondary structure. *In* Circular Dichroism and Conformational Analysis of Biomolecules. G. P. Fasman, editor. Plenum Press, New York. 69–109.

Wishart, D. S., C. G. Bigam, J. Yao, F. Abildgaard, H. J. Dyson, E. Oldfield, J. L. Markley, and B. D. Sykes. 1995. 1H, 13C and 15N chemical shift referencing in biomolecular NMR. *J. Biomol. NMR.* 6:135–140.

Woody, R. W., and A. K. Dunker. 1996. Aromatic and cysteine side chain circular dichroism in proteins. *In* Circular Dichroism and Conformational Analysis of Biomolecules. G. P. Fasman, editor. Plenum Press, New York. 109–158.

Xie, D., and E. Freire. 1994. Structure based prediction of protein folding intermediates. *J. Mol. Biol.* 242:62–80.